



New powder metallurgy preparation method of homogeneous and isomeric Al–Cu–Mg mixed crystal materials

Tao YU¹, Feng LI^{1,2}, Ye WANG², Xue-wen LI³

1. School of Materials Science and Chemical Engineering, Harbin University of Science and Technology, Harbin 150040, China;
2. Key Laboratory of Advanced Manufacturing and Intelligent Technology, Ministry of Education, Harbin University of Science and Technology, Harbin 150040, China;
3. Key Laboratory for Light-weight Materials, Nanjing Tech University, Nanjing 211816, China

Received 1 November 2021; accepted 4 March 2022

Abstract: A new idea of homogeneity isomerism is proposed in this work to break through the single restriction that traditional homogeneous powder metallurgy materials take refining particles as the only modification method. AA2024 alloy powders of different diameters are mixed in a certain proportion through low-energy ball milling, and then a kind of mixed crystal material is successfully fabricated by hot pressing sintering. The results show that the grain morphology of the traditional sample sintered with single-diameter particles tends to become irregular polygon shape, while the grain morphology of the mixed crystal materials forms a special structure in which larger grains are coated with smaller grains. Compared with the former, when the proportion of coarse particles is 20% (mass fraction), the tensile strength increases by 38.8%; when the proportion of coarse particles is 50%, the elongation increases by 14%. The mixed crystal material exhibits a mixed fracture mechanism of intergranular fracture and transgranular fracture, and the pinning effect of the second phase on the dislocation is more obvious, so the properties of the alloy are improved significantly. The above research provides a new idea for the preparation of high-performance homogeneous isomeric mixed crystal materials.

Key words: homogeneous isomerism; Al–Cu–Mg alloy; mixed crystal; powder metallurgy

1 Introduction

Aluminum–magnesium and other light alloy materials have received more and more attention due to their excellent properties and great development potential [1–4]. High-strength 2xxx series aluminum alloys represented by Al–Cu–Mg alloys are widely used in aerospace, rail transit and other fields because of their advantages of low density, high strength, good thermal conductivity, and excellent corrosion resistance [5]. One of the long-term spots of research on the comprehensive

performance of 2xxx series aluminum alloys is how to improve the strength, plasticity, toughness, heat resistance and corrosion resistance of the alloy [6,7]. For metal materials, how to resolve the conflict between strength and plasticity and obtain a metal structural material with a good balance of strength and plasticity becomes one of the effective ways to solve the major scientific problems in this field [8–10].

In recent years, domestic and foreign scholars have broken the traditional design concept of “grain refinement” on improving material performance, and prepared some homogeneous and isomeric

Corresponding author: Feng LI, Tel: +86-13303668051, E-mail: fli@hrbust.edu.cn;
Xue-wen LI, Tel: +86-15124505060, E-mail: lixuewen2000@163.com

DOI: 10.1016/S1003-6326(22)66113-2

1003-6326/© 2023 The Nonferrous Metals Society of China. Published by Elsevier Ltd & Science Press

metal structure materials with cross-scale grains, including the bimodal and multimodal grain structure [11,12], gradient nanostructure [13], heterogeneous lamella structure [14] and other grain structure forms. The preparation methods of mixed crystals mainly include one-step method and two-step method [15]. According to the formation mechanism of the microstructure, the one-step method can be divided into two modes: annealing coarsening and local grain refinement [16]. The method of annealing coarsening is that a homogeneous structure is prepared through severe plastic deformation firstly [17], and then a mixed crystal structure can be obtained through short-time annealing. Local refinement [18] is to control the degree of plastic deformation, so that parts of the grains are refined to ultra-fine crystals or nanocrystals and form a heterogeneous structure. The two-step method is to mix powders of different particle sizes firstly and then combine with various forming technologies, such as spark plasma sintering (SPS) and hot pressing sintering (HPS) to prepare a mixed crystal structure.

WANG et al [19] prepared pure copper with bimodal distribution structure by the method of rolling combined with instant annealing, and its microstructure is characterized by micron-level coarse grains embedded in ultra-fine grains (less than 300 nm) matrix. Its strength is as high as 430 MPa, which is slightly lower than that of nanocrystalline pure copper, but its elongation at break of 65% is close to that of annealed coarse-grained copper.

ZHOU et al [20] obtained a heterogeneous layered structure in 316L stainless steel by a method of large deformation cold rolling and annealing. The structure is characterized by a layered structure composed of coarse-grained and

nanocrystalline/nano-twinned sandwich structures, with a yield strength of 1 GPa, a maximum hardness of HV 530, and an elongation of 20%.

LIDDICOAT et al [21] obtained 10 nm nanocrystals in commercial 7075 aluminum alloy by means of high pressure torsion, and the crystals contained subnanometer solute clusters and two kinds of geometric intra-crystalline nanostructures. The tensile strength of the treated alloy is close to 1 GPa while maintaining a uniform elongation of 4.85%.

It can be seen from the above that the preparation of the mixed crystal structure is an effective way to improve the shaping ability and modification of metal materials, and it is also one of the research hot spots in recent years. In this paper, we put forward a new concept of “homogeneity and isomerism” and a new method based on powder metallurgy to prepare mixed crystal structure billets. Homogeneity refers to the same material, while isomerism refers to the formation of different structures in the same material. In this study, different mixed crystal structures were prepared by adjusting the ratio of the same alloy powders of different diameters. And then a mixed crystal billet with an excellent balance of strength and plasticity was obtained, which will have an important influence on the microstructure and properties of subsequent formed products.

2 Experimental

2.1 Technical principle

In this study, the mixed crystal structure was prepared by the two-step method, and the process principle is shown in Fig. 1. At first, the two original alloy powders of different diameters were mixed uniformly by low-energy ball milling, and

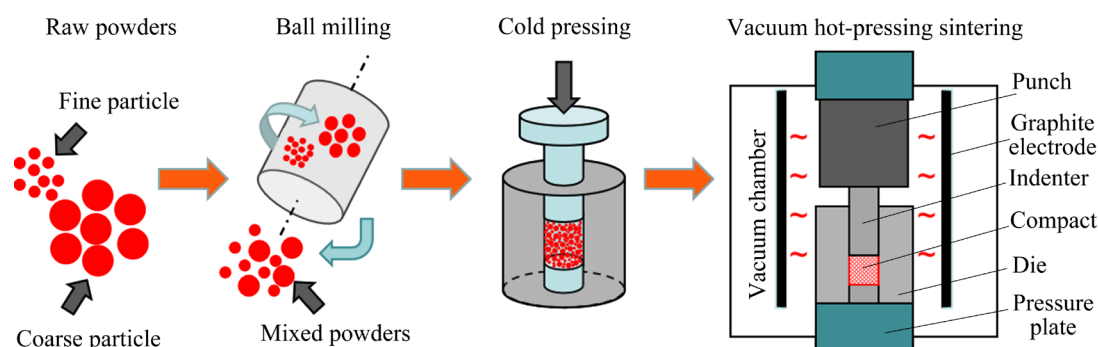


Fig. 1 Schematic diagram of preparation process of powder mixed crystal

then the mixed powders were pressed into a compact by a unidirectional compression molding method. Finally, the compact was sintered in the vacuum hot pressing sintering furnace. Two kinds of powders of different diameters were organically combined together under the conditions of high temperature and pressure, and then a kind of homogeneous and isomeric alloy material with a balance of strength and plasticity was prepared in this way.

The advantage of the method lies in that the microstructure of the mixed crystal billet can be controlled precisely by changing the ratio of the powders of different diameters according to the requirements.

2.2 Experimental procedures

AA2024 alloy powders used in this study were produced by a nitrogen atomization technique, and the average diameters of the powders were selected as 10 and 40 μm , respectively. The main chemical components of the alloy powders are shown in Table 1.

Table 1 Chemical composition of AA2024 alloy powder (mass fraction, %)

Cu	Mg	Si	Ti	Cr	Fe	Mn	Zn	Al
4.11	1.64	0.15	0.02	0.01	0.21	0.81	0.07	Bal.

According to the mass ratio of coarse to fine particles 0:1 (1[#]), 2:8 (2[#]), 5:5 (3[#]) and 8:2 (4[#]), powders of different diameters were weighed in a glove box filled with argon. And then, the planetary ball mill was used for low-energy ball milling mixing under the nitrogen atmosphere (220 r/min, 5 h, mass ratio of ball to material of 3:1, and the diameter of the hard alloy steel ball of 5 mm). Before mixing, the ball milling tank and the steel balls should be cleaned up with alcohol to prevent impurities. And the raw material powders should also be taken out from the glove box and stored in the vacuum package for later use. Then, a $d40\text{ mm} \times 34\text{ mm}$ mixed-crystal compact was prepared by unidirectional compression molding. Finally, the compact was put into a steel die coated with boron nitride (the size of the inner cavity of the die is $d40\text{ mm} \times 100\text{ mm}$) and sintered in a hot pressing sintering furnace. The technological process is shown in Fig. 2: the furnace was heated to 570 °C at a rate of 10 °C/min under the vacuum

condition, and then kept the pressure at 25 MPa and the temperature at 570 °C for 2 h. When the temperature of the furnace was cooled down to room temperature, a $d40\text{ mm} \times 30\text{ mm}$ mixed crystal billet was obtained. The sintered samples were numbered as Alloys 1[#], 2[#], 3[#] and 4[#] according to the amount of the powders with different mass ratios.

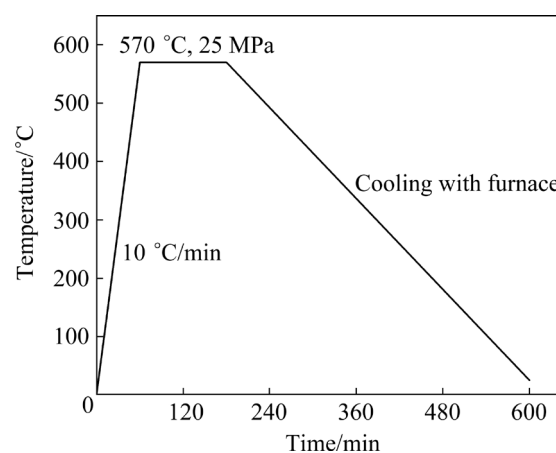


Fig. 2 Hot pressing sintering process

2.3 Microstructure and property characterization

The sintered sample was cold inlaid with epoxy resin. After polishing, the sample was etched with Keller reagent for 20 s, and its microstructure was observed under the optical microscope (OM). S-300 scanning electron microscope (SEM) and energy dispersive spectrometer (EDS) were used to analyze the morphology of 2024 aluminum alloy powders, the distribution of precipitated phases and the microstructure evolution of the sintered sample. The composition of the phases of the sintered sample was tested and analyzed under the X'Pert PRO X-ray diffractometer. The mechanical properties of the sintered samples were tested by an Instron 5569 universal tester with a strain rate of $1 \times 10^{-3}\text{ s}^{-1}$ and a tensile rate of 1 mm/min. And then the fracture morphology of the tensile samples was observed under the scanning electron microscope.

3 Results and discussion

3.1 Powder morphology and composition

The comparison of the morphology of original powders and powders mixed with different diameters is shown in Fig. 3. And Figs. 3(a)–(d) also exhibit the distribution of 1[#], 2[#], 3[#], and 4[#] powders.

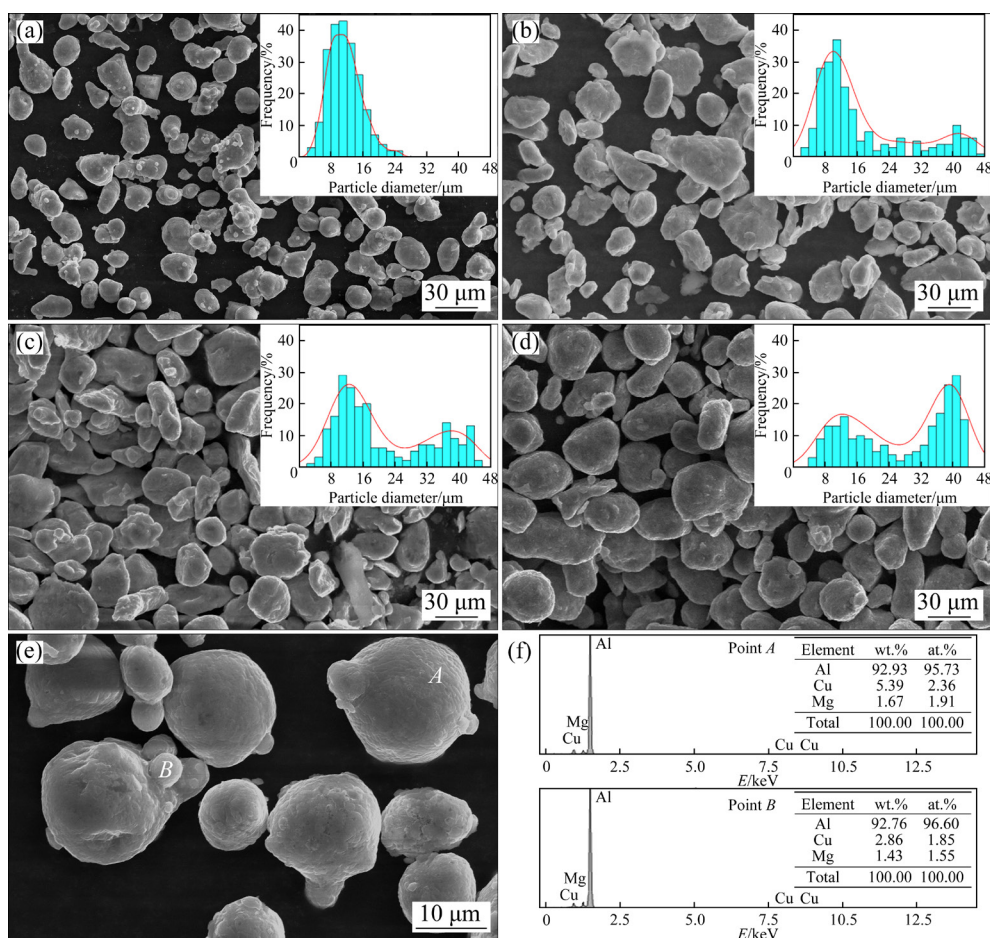


Fig. 3 Comparison of morphology of Samples 1[#]–4[#] mixed with different diameters (a–d), respectively, and morphology (e) and EDS results (f) of original powders

It can be seen from Fig. 3(a) that the original aluminum alloy powders prepared by the nitrogen atomization technique are ellipsoidal and rod-shaped, and the powders are in different sizes and shapes. The smaller particles are adhered to the surface of the larger particles to form “satellite particle”. The morphology and the EDS results of the original powders are shown in Fig. 3(e), which shows the surface morphology of the original particle and the distribution of small particles. Smaller particles were attached to the surface of larger particles, and some smaller particles even had fused with larger particles and form mountain-shaped protrusions. This is because in the process of preparing powders by nitrogen atomization technique, the metal liquid was broken into countless small droplets of different sizes under the action of impact force. The smaller metal droplets took the lead in solidification due to their larger surface tension and undercooling degree. Because of their smaller diameter and fast

movement, smaller particles were adhered to the surface of larger particles and formed smaller “satellite particles” when they collided with larger metal droplets. Through the energy spectrum of the original powders, it can be seen that the element composition of the smaller and larger powders is basically same, and the contents of other alloying elements such as Cu are not obvious. It is speculated that Cu and other alloying elements are dissolved in Al.

From Figs. 3(b)–(d), it can be seen that after the powders of different diameters were mixed in three different proportions, the mixed powders produced a certain degree of plastic deformation because of the impact of the grinding balls. The shape of the particles became irregular, and the larger ellipsoidal particles became flat [22]. Some smaller particles fused together to form new particles, and the smaller “satellite particles” basically disappeared.

Through the comparison of the distribution of

the particle diameter in Figs. 3(a)–(d), the difference between the powders with different mass ratios can be more clearly seen. The average diameter of the original powders is concentrated at around 10 μm , but the diameter distribution curve of the mixed powders shows different peaks. Due to the difference between the diameters, some fine powders can also be seen in the original coarse powders. As the proportion of coarse powders increases, the wave peak of the coarse powders does not change significantly.

Figure 4 shows the XRD patterns of the powders mixed with different mass ratios. It can be

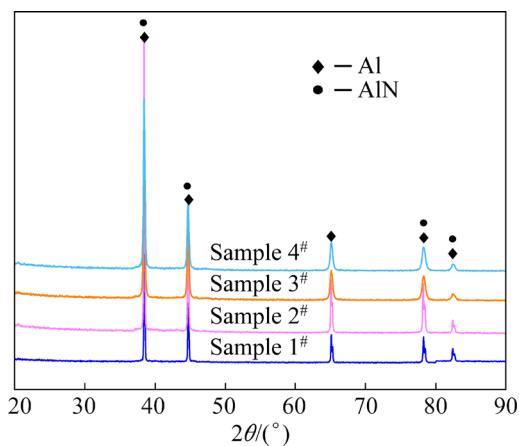


Fig. 4 XRD patterns of powders mixed with different mass ratios of coarse and fine powders

seen from Sample 1[#] that the AA2024 alloy powder prepared by the nitrogen atomization technique is mainly composed of $\alpha(\text{Al})$ and AlN phases, and no diffraction peaks of other elements appear. The XRD pattern further indicates that Cu, Mg, Mn and other elements are almost dissolved in Al, which also verifies the previous speculation. After low-energy ball milling, the phases of Samples 2[#], 3[#] and 4[#] do not change significantly, and there are no new diffraction peaks. Compared with Sample 1[#], the diffraction peaks of the mixed powders are wider. The broadening of diffraction peaks is mainly caused by the refinement of grain and the increase of microscopic strain. In the process of low-energy ball milling, the collision of the grinding balls causes part of the powders to be broken and the crystal grains are refined. There are two main reasons for the change of microscopic strain. On the one hand, the low-energy ball milling process promotes the solid solution of other alloying elements. On the other hand, the plastic deformation of the powders during the ball milling process will also cause the increase of microscopic strain. Therefore, the ball milling process promotes the refinement and homogenization of powders.

3.2 Microstructure

Figure 5 shows the comparison of the micro-

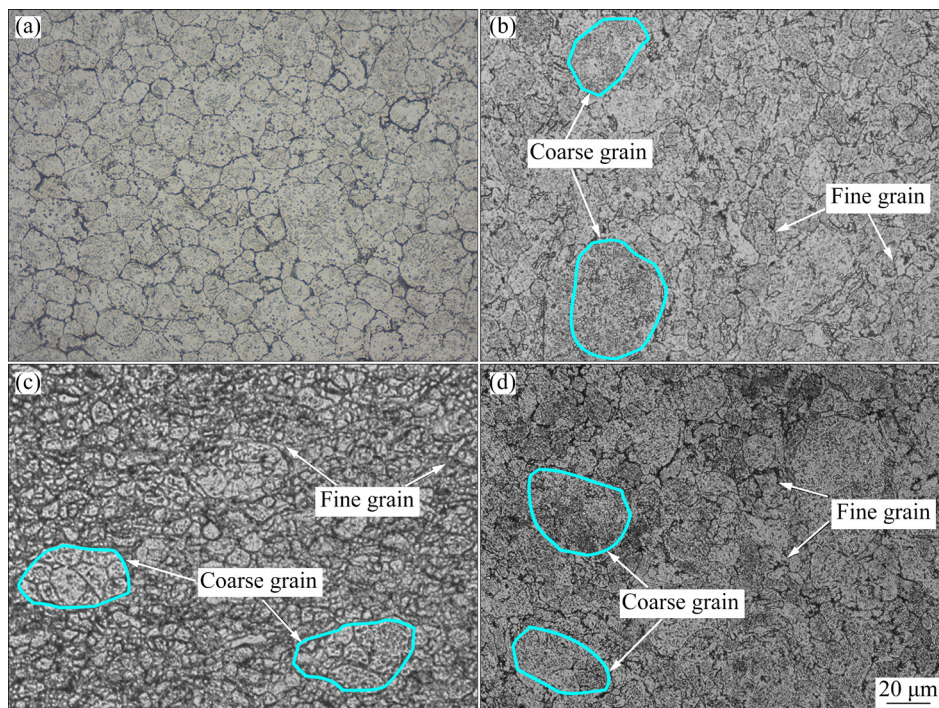


Fig. 5 Microstructures of samples sintered with different mass ratios of powders: (a) Sample 1[#]; (b) Sample 2[#]; (c) Sample 3[#]; (d) Sample 4[#]

structure of the samples sintered with different mass fractions of powders.

It can be seen from Fig. 5 that as the proportion of coarse powders increases, the difference in grain size was more significant. In Fig. 5(a), the grains were uniform, and the grains tended to become irregular polygons. While in Figs. 5(b)–(d), most of the original particles were fused together during the sintering and the boundaries of particles became blurred. The smaller unfused original particles were wrapped around the larger particles to form a special stepped structure.

It can be seen from Fig. 3 that the shape of the raw powders and mixed powders were obviously different. The powders without low-energy ball milling basically remained a round and full shape and the diameter was uniform. When the powders suffered a certain degree of plastic deformation, the difference between particles became more obvious. In order to reduce the surface energy, the grain boundaries tended to be flat and reduced the surface area under the condition of high temperature and pressure. The smaller the particle diameter is, the finer the gaps between particles will be. And the particle rearrangement will be more difficult, so powders of Sample 1[#] were compacted quickly. For the mixed powders, due to the change of the particle morphology and the difference in particle size, the gaps between the particles are larger than those of the unmixed powders. Under the action of axial pressure during sintering, the smaller particles entered the larger gap [23]. During the process of movement, smaller particles were swallowed by larger particles, and the boundaries of the fused particles became smooth, while the other unfused smaller particles were coated around the larger particles to form a special structure. And then a multi-scale crystal grain structure formed, as the coarse and fine grain regions shown in Figs. 5(b)–(d).

The black part between grain boundaries in Fig. 5 was preliminarily judged to be the second phase Al_2Cu [24], and Fig. 6 shows an XRD comparison of sintered samples. The diffraction peaks of Al_2Cu can be clearly seen in Fig. 6, and as the mass fraction of the coarse powders increases, the diffraction peaks of Al_2Cu become sharp, which indicates that the precipitated phases become coarse and concentrated and also confirms the previous judgment.

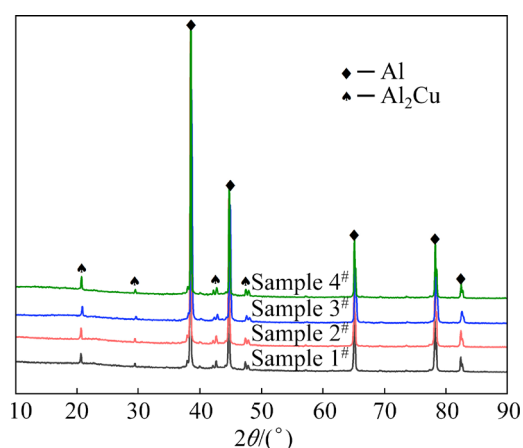


Fig. 6 XRD patterns of samples sintered with different mass ratios of powders

3.3 SEM observation

In order to further analyze the microstructure of the sintered samples, the sintered alloy samples were analyzed by SEM and EDS. SEM images of the sintered samples are shown in Fig. 7.

There are some pores between the grain boundaries of Sample 1[#] in Fig. 7(a), while the number of the pores is reduced obviously in Sample 2[#], 3[#] and 4[#] in Figs. 7(b)–(d), respectively. The number of the pores is related to the original shape of particle. Because of small difference in particle size and shape of powders in Sample 1[#], and as the powders did not achieve complete liquid phase when sintered at 570 °C, the fine gaps between particles made particle rearrangement difficult and the density of Sample 1[#] low. However, the mixed powders have suffered a certain degree of predeformation and the particle diameter varies greatly, so different particle shapes promote the powders to coordinate with each other, which also facilitate the sintering process [25]. Under the condition of external force, small particles are more likely to enter the gaps between particles, and the rearrangement of particles is relatively easy, which can further form a mixed crystal structure. Therefore, under the same sintering conditions, the samples sintered with different mass ratios of powders will have a higher density.

By comparing the images in Fig. 7, it can be easily found that the bright white θ phases are distributed uniformly in Samples 1[#], 2[#], 3[#] and 4[#]. The size and the shape of the second phases are different. In addition, the needle-shape S phase (Al_2CuMg) with a certain direction can also be seen

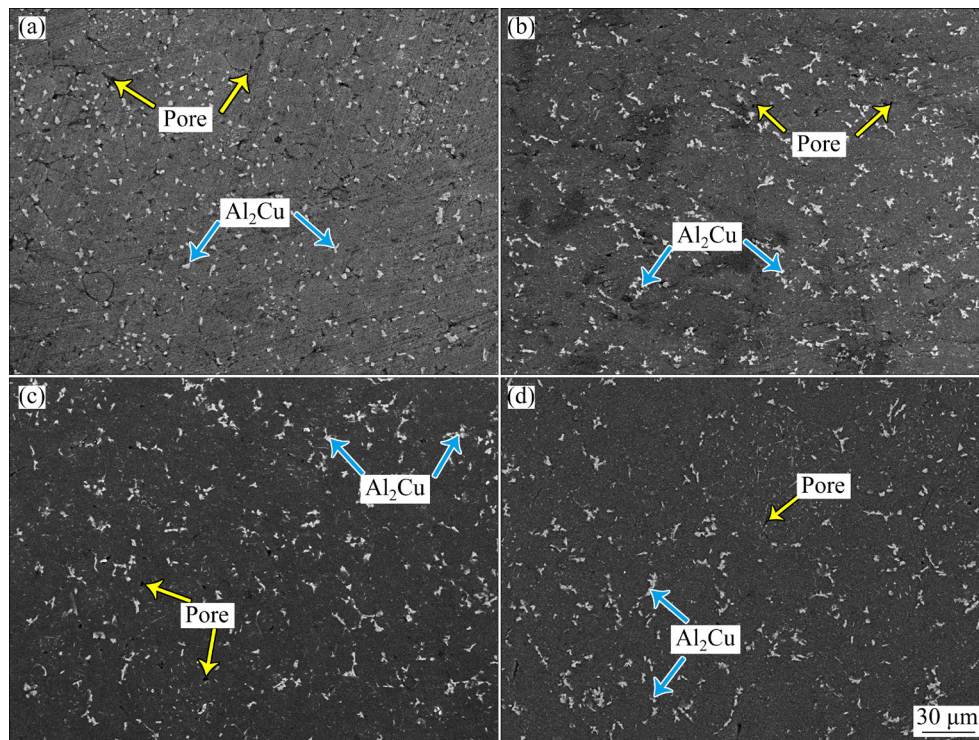


Fig. 7 SEM images of samples sintered with different mass ratios of powders: (a) Sample 1[#]; (b) Sample 2[#]; (c) Sample 3[#]; (d) Sample 4[#]

inside the grains. The high density *S* phase precipitated inside the grains will have a significant strengthening effect on the properties of the alloy [26]. The precipitated phases of Sample 1[#] in Fig. 7(a) are mainly θ phase (Al_2Cu), and most of the phases are continuously distributed along the grain boundaries in dot shape. The distributions of the precipitated phases are dense and uniform, though a few precipitated phases still exist inside the grains. During the sintering process of Sample 1[#], the grain boundaries gradually melt as the temperature rises. Due to the high energy at the grain boundary, it will be easier to satisfy the eutectic condition at the grain boundary than inside the grain, and the Al–Cu eutectic liquid phase is formed first. During the cooling process, the intermetallic compound Al_2Cu is precipitated from the eutectic liquid phase at a temperature of 548 °C. Because of the small difference of particles, the grain boundaries tend to be straight, and the precipitated Al_2Cu fully fills the gaps between particles, thus the second phases exhibit a dot-like and continuous distribution along grain boundaries. This kind of distribution of precipitated phases will make the particles fail to form an effective diffusion connection, which will greatly affect the

mechanical properties of the alloy.

It can be seen from Figs. 7(b)–(d) that the morphologies of precipitated phase in sintered Samples 2[#], 3[#] and 4[#] are different from that of Sample 1[#]. The dot-like precipitated phases become flocculent, and the precipitated phases are mostly distributed at the three-way intersection of grains. As the difference in size of particles increases, the grains are no longer blocked by the dot-like precipitated phase, and the flocculent precipitated phases penetrate into the inside of the particles and strengthen the diffusion and bonding between the particles, so that the combination between the particles is more uniform and compact. And as the mass fraction of coarse particles increases, the distribution of flocculent precipitated phases gradually becomes sparse. Because large particles are more likely to deform under the pressure, the pores between particles become elongated. The high energy at the particle boundary makes the second phases precipitate along the boundary preferentially and fill the gaps between particles, so the shape of the second phase becomes flocculent. Finally, the observable grains in the same area are reduced relatively, and the coarse precipitated phases are sparse.

3.4 Element distribution

In order to further analyze the composition of the precipitated phases and the basic law of element diffusion, the EDS results of Samples 1[#], 2[#], 3[#], and 4[#] are shown in Fig. 8.

From the elemental mapping images in Figs. 8(a)–(d), it can be further confirmed that the main component of the precipitated phases is Al_2Cu . The content of Mg in the energy spectrum is very low, even no obvious Mg element is detected.

However, the elemental mapping of Mg and the high-power scanning electron microscope images in Figs. 8(a)–(d) confirm the existence of needle-like S phase (Al_2CuMg) inside the particle. It can also be seen from the elemental mapping in Fig. 8 that the area of white phases in the alloy is the enriched area of Cu, Mg and other elements, and the number of the second phases at the grain boundary is obviously more than that inside the grain. It can be seen from Fig. 7 that as the mass fraction of coarse

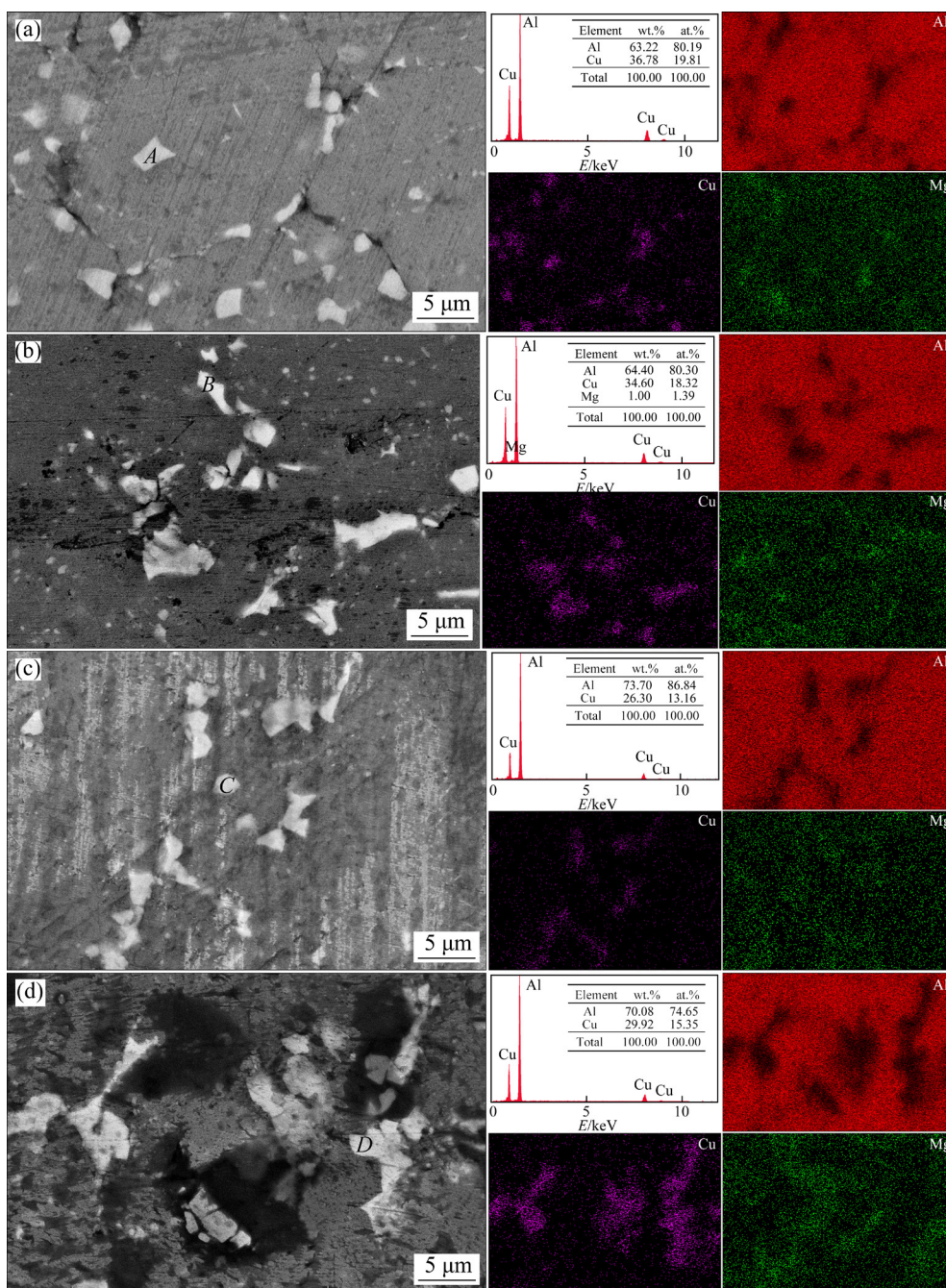


Fig. 8 Elemental mappings of samples sintered with different mass ratios of powders: (a) Sample 1[#]; (b) Sample 2[#]; (c) Sample 3[#]; (d) Sample 4[#]

particles increases, the precipitated phases in grains gradually increase, and the precipitated phases inside the large grains are finer and more uniform. This phenomenon showed that during the sintering process, Cu and Mg elements concentrated in the gaps between grain boundaries and caused element segregation [27]. Some elements failed to completely diffuse to the grain boundary, and formed dispersedly distributed precipitated θ and S phases inside the grains. Due to the difference in particle size, the diffusion of alloying elements in small particles is faster than that in large particles, and it took less time for alloying elements to diffuse from high-concentration points inside the grain to low-concentration grain boundary. Therefore, as the mass fraction of coarse particles increases, the residual second phases inside the grain become denser.

3.5 Mechanical properties

Several $\phi 40 \text{ mm} \times 2 \text{ mm}$ discs were cut from the sintered samples at the same position, and then they were processed them into bone-like tensile samples. The tensile properties of sintered samples were tested on the Instron 5569 universal testing machine at a strain rate of $1 \times 10^{-3} \text{ s}^{-1}$ and a tensile rate of 1 mm/min. Take the average value after 3 times of tensile test for each sample. The comparison of the tensile strength and elongation of the samples sintered with different mass ratios of powders is shown in Fig. 9.

The tensile strength and elongation of the Sample 1[#] with a coarse to fine powder mass ratio of 0:1 are relatively general, with a tensile strength of 140.3 MPa and an elongation of 8.8%. After mixing the coarse and fine powders in a certain proportion, the elongation value of the sintered sample increases obviously. Sample 2[#] with a mass fraction (20%) of coarse powders increases its tensile strength by 38.9% to 194.9 MPa, and its elongation reached 11.8%. When the mass fraction of coarse powders reaches 50%, the tensile strength of Sample 3[#] decreases to 180.3 MPa, but its elongation further increases to 22.8%. The reason is that the strength and plasticity of metals are the result of the interaction of coarse and fine grains [28]. The phenomenon in this special mixed crystal structure with fine grains encapsulating coarse grains is particularly evident.

The deformation mechanism of the mixed

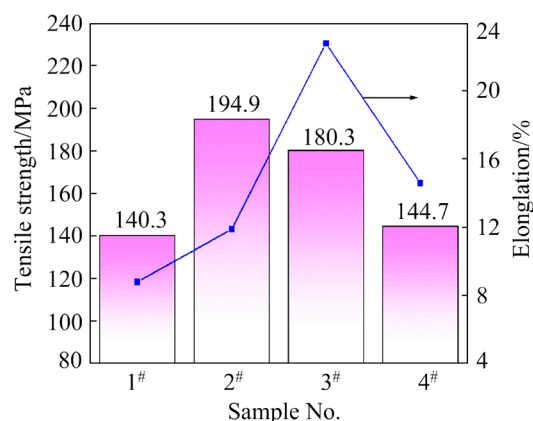


Fig. 9 Comparison of tensile strength and elongation of samples sintered with different mass ratios of powders

crystal structure is caused by synergistic effect of the soft phase composed of coarse grains and the hard phase composed of fine grains, which is much more complicated than the traditional uniform structure. In the mixed crystal structure, there are not only a difference in spatial orientation among the grains, but also a difference in grain size, which will lead to non-uniform distribution of stress and strain. Firstly, elastic deformation occurs in soft and hard phases simultaneously. Then, the soft phase yields but the hard phase remains elastic. Finally, both the soft phase and the hard phase proceed to the plastic deformation stage. In the three deformation stages of mixed crystal materials, the soft phase bears most of the strain, which can better coordinate the deformation of the matrix and make the whole strain uniform. On the other hand, the back stress strengthening caused by the interaction of the coarse grains and fine grains greatly improves the strain hardening ability and the strength of the soft phase.

Therefore, the mixed crystal structure has an excellent balance of strength and plasticity. However, when the proportion of coarse particles is too high, the strength of the material will significantly decrease and the sample will break prematurely during the tensile test. For example, when the proportion of coarse particles further increases to 80%, the tensile strength of Sample 4[#] decreases obviously and breaks prematurely, with an elongation of 14.6%. Though the soft phase provides better coordinated deformation ability, it also causes the contact area between particles to become larger. And the crack source at the pores will spread faster, which makes the performance of

Sample 4[#] worse. In summary, when the proportion of coarse particles is 50%, the alloy will possess a good balance of strength and plasticity.

3.6 Fracture morphology and fracture mechanism

Figures 10(a) and (b) show the comparison of tensile fracture with the mass ratio of coarse and fine particles of 0:1 and 5:5, respectively. The morphological characteristics of the original powder can still be seen from Fig. 10(a). Because of the difference in particle size, the billet is not completely dense [29]. At 570 °C, the Al particles are only partially liquefied, and the sintering necks formed between the particles are small, so the bonding between the particles is only through the growth and diffusion connection of the sintering necks under high temperature and pressure. The particles are not completely fused together, so the original powder morphology can be seen clearly. In Fig. 10(a), there are obvious gaps between grains, and there are a large number of dot-like precipitated phases (Al_2Cu) at grain boundaries. The second phase at the gaps between grains will become the source of fracture when the material cracks, which is one of the important reasons for the poor mechanical properties of Sample 1[#]. The fracture morphology of Sample 3[#] in Fig. 10(b) shows that although there are still gaps between the grains, the distribution of coarse and fine grains is relatively uniform. Smaller grains are densely distributed around larger grains, and the white phases at grain boundaries fully fill the gaps between the grains and penetrate into the interior of the grains, which makes the binding between the grains closer.

The tensile fracture of Fig. 10(a) shows that the fracture mode of Sample 1[#] is peeling along the grain gaps and exhibits intergranular fracture. On the other hand, the tensile fracture of Sample 3[#] shown in Fig. 10(b) is characterized by the transgranular fracture in some areas, and some traces of ravines can be observed. This is because the precipitated phase (Al_2Cu) embedded in the grains hinders dislocation motion and improves the alloy in tensile.

For Sample 1[#], due to the concentration of the local stress and strain near grain boundary in the tensile deformation process, the energy at the boundary will be several times higher than that inside the grain, and it is difficult for the grain to effectively accumulate dislocations and release

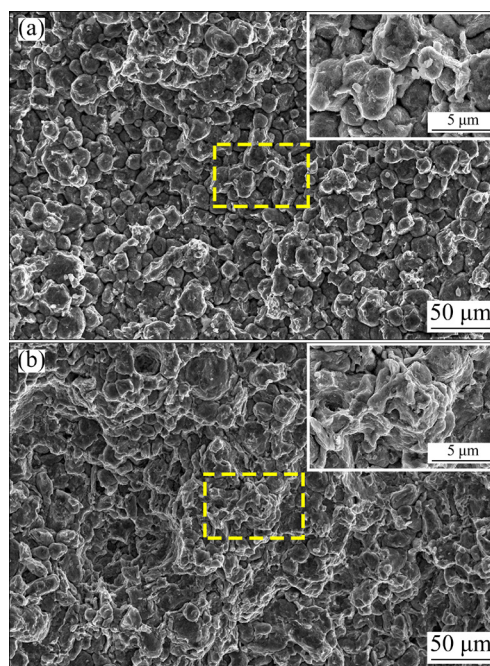


Fig. 10 Comparison of fracture morphologies of samples sintered with different mass ratios of powders: (a) Sample 1[#]; (b) Sample 3[#]

them on microscale [30]. Moreover, the second phases in Sample 1[#] are continuously distributed along the grain boundaries in dot shape, and the pinning effect on the dislocation is not obvious, which greatly reduces the uniform deformation ability of the material and causes the material to peel off along the gaps between grain boundaries. The coarse grain phase and the fine grain phase in Sample 3[#] are coordinated with each other and the strengthening effect of second phases is obvious, so the material possesses a higher tensile strength.

Compared with Samples 2[#] and 3[#], Sample 4[#] has a better plasticity and a lower strength. Because there exist more coarse particles in Sample 4[#], the grain size of Sample 4[#] is larger. Although the pinning effect makes a contribution to the deformability, the cracks spread faster along the gaps because of the relatively large contact surface between grains, which results in the fact that the fracture of the alloy occurs prematurely.

4 Conclusions

(1) A new method on the preparation of homogeneous isomeric materials is proposed based on powder metallurgy. And a kind of mixed crystal billet with an excellent balance of strength and

plasticity is successfully prepared. By the new method, a special structure in which larger grains are coated with smaller grains is generated in the sintered sample, and the sintered sample has a higher degree of densification.

(2) AA2024 alloy samples sintered with hot pressing have a large number of precipitated phases. In the sample sintered with single-diameter particles, the precipitated phases are mostly distributed along the grain boundaries in dot shape. And the reaction between second phases and dislocations is limited. While in the sample sintered with mixed powders, the shape of precipitated phases becomes flocculent and the second phases are embedded in the grains to hinder dislocation motion. In addition, due to the difference in particle size, the residual precipitates are formed inside the large grains and enhance the performance of the alloy.

(3) Compared with the traditional hot-pressing sintering AA2024 alloy material, the comprehensive performance of mixed crystal AA2024 aluminum alloy is better. Compared with the former, when the proportion of coarse particles is 20%, the tensile strength reaches 194.9 MPa, which increases by 38.9%. When the proportion is 50%, the elongation is further improved and reaches 22.8%, increased by 14%.

(4) The fracture mechanism of the AA2024 aluminum alloy sample sintered with single-diameter particles is mainly intergranular fracture. The mixed crystal materials exhibit a mixed fracture mechanism of intergranular fracture and transgranular fracture. The difference of the fracture mechanism also shows that the property of the mixed crystal material is better.

Acknowledgments

This work was supported by the Key Laboratory of Micro-systems and Micro-structures Manufacturing of Ministry of Education, Harbin Institute of Technology, China (No. 2020KM005), and the Natural Science Foundation of Heilongjiang Province, China (No. YQ2020E030).

References

[1] HUANG K, ZHANG K, MARTHINSEN K, LOGE R E. Controlling grain structure and texture in Al–Mn from the competition between precipitation and recrystallization [J]. *Acta Materialia*, 2017, 141: 360–373.

[2] WANG Ye, ZHANG Shun, WU Rui-zhi, TURAKHODJAEV N, HOU Le-gan, ZHANG Jing-huai, BETSOFEN S. Coarsening kinetics and strengthening mechanisms of core-shell nanoscale precipitates in Al–Li–Yb–Er–Sc–Zr alloy [J]. *Journal of Materials Science & Technology*, 2021, 61: 197–203.

[3] WANG Ye, LI Feng, BIAN Nan, XIAO Xing-mao. Coordinated control of preferred orientation and uniformity of AZ31 in accumulative alternating back extrusion [J]. *Materials Science and Engineering A*, 2021, 818: 141366.

[4] HE Ying-jie, XU Hong-yu, JIANG Bo, JI Ze-sheng, HU Mao-liang. Microstructure, mechanical and tribological properties of (APC+B₄C)/Al hybrid composites prepared by hydrothermal carbonized deposition on chips [J]. *Journal of Alloys and Compounds*, 2021, 888: 161578.

[5] DURSUN T, SOUTIS C. Recent developments in advanced aircraft aluminium alloys [J]. *Materials & Design*, 2014, 56: 862–871.

[6] EVAN M A, ZHU T. Towards strength–ductility synergy through the design of heterogeneous nanostructures in metals [J]. *Materials Today*, 2017, 20: 323–331.

[7] FAN Cai-he, OU Ling, HU Ze-yi, YANG Jian-jun, CHEN Xi-hong. Re-dissolution and re-precipitation behavior of nano-precipitated phase in Al–Cu–Mg alloy subjected to rapid cold stamping [J]. *Transactions of Nonferrous Metals Society of China*, 2019, 29(12): 2455–2462.

[8] OVID'KO I A, VALIEV R Z, ZHU Y T. Review on superior strength and enhanced ductility of metallic nanomaterials [J]. *Progress in Materials Science*, 2018, 94: 462–540.

[9] CHEN Liang, ZHAO Guo-qun, YU Jun-quan, ZHANG Wen-dong. Constitutive analysis of homogenized 7005 aluminum alloy at evaluated temperature for extrusion process [J]. *Materials & Design*, 2015, 66: 129–136.

[10] LI Yu-qiang, CHEN Liang, TANG Jian-wei, ZHAO Guo-qun, ZHANG Cun-sheng. Effects of asymmetric feeder on microstructure and mechanical properties of high strength Al–Zn–Mg alloy by hot extrusion [J]. *Journal of Alloys and Compounds*, 2018, 749: 293–304.

[11] HAN B Q, HUANG J Y, ZHU Y T, LAVERNIA E J. Strain rate dependence of properties of cryomilled bimodal 5083 Al alloys [J]. *Acta Materialia*, 2006, 54(11): 3015–3024.

[12] LI Xin-yu, XIA Wei-jun, CHEN Ji-hua, YAN Hong-ge, LI Zhen-zhen, SU Bin, SONG Min. Dynamic recrystallization, texture and mechanical properties of high Mg content Al–Mg alloy deformed by high strain rate rolling [J]. *Transactions of Nonferrous Metals Society of China*, 2021, 31(10): 2885–2898.

[13] LU Ke. Gradient nanostructured materials [J]. *Acta Metallurgica Sinica*, 2015, 51(1): 1–10.

[14] WU Xiao-lei, YANG Mu-xin, YUAN Fu-ping, WU Guilin, WEI Yu-jie, HUANG Xiao-xu, ZHU Yun-tian. Heterogeneous lamella structure unites ultrafine-grain strength with coarse-grain ductility [J]. *Proceedings of the National Academy of Sciences of the United States of America*, 2015, 112(47): 14501–14505.

[15] ZHA Min, ZHANG Hong-min, YU Zhi-yuan, ZHANG Xuan-he, MENG Xiang-tao, WANG Hui-yuan, JIANG Qi-chuan. Bimodal microstructure—A feasible strategy for

- high-strength and ductile metallic materials [J]. *Journal of Materials Science & Technology*, 2018, 34(2): 257–264.
- [16] VALIEV R Z, SERGUEEVA A V, MUKHERJEE A K. The effect of annealing on tensile deformation behavior of nanostructured SPD titanium [J]. *Scripta Materialia*, 2003, 49(7): 669–674.
- [17] ESTRIN Y, VINOGRADOV A. Extreme grain refinement by severe plastic deformation: A wealth of challenging science [J]. *Acta Materialia*, 2013, 61(3): 782–817.
- [18] ZHENG Rui-xiao, BHATTACHARJEE T, SHIBATA A, SASAKI T, HONO K, JOSHI M, TSUJI N. Simultaneously enhanced strength and ductility of Mg–Zn–Zr–Ca alloy with fully recrystallized ultrafine grained structures [J]. *Scripta Materialia*, 2017, 131: 1–5.
- [19] WANG Yin-min, CHEN Ming-wei, ZHOU Feng-hua, MA En. High tensile ductility in a nanostructured metal [J]. *Nature*, 2002, 419(6910): 912–915.
- [20] ZHOU Zhong-chen, WANG Shuai-zhuo, LI Jian-sheng, LI Yu-sheng, WU Xiao-lei, ZHU Yun-tian. Hardening after annealing in nanostructured 316L stainless steel [J]. *Nano Materials Science*, 2020, 2: 80–82.
- [21] LIDDICOAT P V, LIAO Xiao-zhou, ZHAO Yong-hao, ZHU Yun-tian, MURASHKIN M Y, LAVERNIA E J, VALIEV R Z, RINGER S P. Nanostructural hierarchy increases the strength of aluminium alloys [J]. *Nature Communications*, 2010, 63(1): 1–7.
- [22] GUAN Di-kai, GAO Jun-heng, RAINFORTH W M. Effect of cryomilling time on microstructure evolution and hardness of cryomilled AZ31 powders [J]. *Materials Characterization*, 2021, 178: 111311.
- [23] SCHAFFER G B, HALL B J, BONNER S J, HUO S H, SERCOMBE T B. The effect of the atmosphere and the role of pore filling on the sintering of aluminium [J]. *Acta Materialia*, 2006, 54(1): 131–138.
- [24] GÖKÇE A, FINDIK F, KURT A O. Microstructural examination and properties of premixed Al–Cu–Mg powder metallurgy alloy [J]. *Materials Characterization*, 2011, 62(7): 730–735.
- [25] LIU Z Y, SERCOMBE T B, SCHAFFER G B. The effect of particle shape on the sintering of aluminum [J]. *Metallurgical and Materials Transactions A*, 2007, 38 (6): 1351–1357.
- [26] ZHANG Xue-zheng, CHEN Ti-jun. Bimodal microstructure dispersed with nanosized precipitates makes strong aluminum alloy with large ductility [J]. *Materials & Design*, 2020, 191: 108695.
- [27] DING Li-ping, JIA Zhi-hong, NIE Jian-feng, WENG Yao-yao, CAO Ling-fei, CHEN Hou-wen, WU Xiao-zhi, LIU Qing. The structural and compositional evolution of precipitates in Al–Mg–Si–Cu alloy [J]. *Acta Materialia*, 2018, 145: 437–450.
- [28] GUO X, YANG G, WENG G J. The saturation state of strength and ductility of bimodal nanostructured metals [J]. *Materials Letters*, 2016, 175: 131–134.
- [29] CAI Zhi-yong, ZHANG Chun, WANG Ri-chu, PENG Chao-qun, WU Xiang, LI Hai-pu, YANG Ming. Improvement of deformation capacity of gas-atomized hypereutectic Al–Si alloy powder by annealing treatment [J]. *Transactions of Nonferrous Metals Society of China*, 2018, 28(8): 1475–1483.
- [30] ANTOLOVICH S D, ARMSTRONG R W. Plastic strain localization in metals: origins and consequences [J]. *Progress in Materials Science*, 2014, 59: 1–160.

同质异构 Al–Cu–Mg 系混晶粉末冶金制备新方法

于涛¹, 李峰^{1,2}, 王野², 李学问³

1. 哈尔滨理工大学 材料科学与化学工程学院, 哈尔滨 150040;

2. 哈尔滨理工大学 先进制造智能技术教育部重点实验室, 哈尔滨 150040;

3. 南京工业大学 先进轻质高性能材料研究中心, 南京 211816

摘要: 为突破传统同质粉末材料均以颗粒尺寸细化作为改性的单一途径禁锢, 提出同质异构思想, 即通过低能球磨将不同粒径的 AA2024 合金粉末按照一定比例混合, 经热压烧结制备混晶坯料。研究表明, 传统单一粒径粉末烧结后晶粒形貌趋向于不规则多边形, 而不同粒径粉末混合烧结后晶粒形貌为小颗粒包覆大颗粒的结构形式; 与前者相比, 当粗粉占比为 20%(质量分数)时, 抗拉强度增加了 38.8%; 当粗粉占比为 50%时, 伸长率提高了 14%。粉末混合后的烧结样品呈沿晶断裂和穿晶断裂的混合断裂机制, 第二相对位错的钉扎效应更加明显, 因此, 合金性能得到显著提高。此研究工作为高性能同质异构混晶材料的制备提供了一种新思路。

关键词: 同质异构; Al–Cu–Mg 合金; 混晶; 粉末冶金

(Edited by Wei-ping CHEN)